International Core Journal of Engineering Volume 7 Issue 6, 2021
ISSN: 2414-1895 DOI: 10.6919/ICJE.202106_7(6).0073

New Harmonic Detection of Electric Propulsion Ship based on Improved DOGI-PLL

Yuanrui Zhang[1,a], Weifeng Shi[1,b], Haiming Guo[1,c] and Yi Ding[1,d]

[1]Logistics Engineering College, Shanghai Maritime University, Shanghai 201306, China.

[a]zyr19970813@163.com, [b]wfshi@shmtu.edu.com, [c]1207512538@qq.com, [d]593195572@qq.com

Abstract

Due to the use of nonlinear high-power power electronic equipment such as frequency converter, the harmonic content of marine electric propulsion system is higher. In order to ensure the APF works normally under the condition of three-phase unbalance, grid distortion or harmonic pollution, PLL with high performance needs to detect the phase and frequency of the positive sequence component of the voltage base frequency of the power grid quickly and accurately. Traditional p-q and ip-iq detection algorithms based on instantaneous reactive power theory, The harmonic suppression ability of PLL based on synchronous reference frame (SFR-PLL) is poor, which can not meet the requirements. A software phase locked loop algorithm with double generalized second order integrators (DSOGI-PLL) is proposed. The simulation results show that the method can avoid the influence of negative sequence component in voltage and has strong tracking effect on harmonic detection.

Keywords

Marine Electric Propulsion System; Harmonic; PLL; APF; Second Order Generalized Integrator.

1. Introduction

In the marine electric propulsion system, the harmonic detection of traditional active power filter (APF) relies on the performance of phase-locked loop which is synchronized with the power grid. In order to ensure the reliable operation of APF, the grid voltage can not be regarded as a constant amplitude. It is necessary to continuously monitor the amplitude, frequency and phase of grid voltage to ensure the coordination between APF and marine electric propulsion unit grid I want to do my job. Phase locked loop (PLL) can automatically track the phase and frequency of input signal and output phase synchronization signal. Therefore, in the power grid detection, using phase-locked technology for real-time detection of power grid state is the current method to realize the harmonic detection of active power filter and the synchronization of propulsion unit power grid. During the operation of ship propulsion system, there may be various faults, such as voltage sag, voltage imbalance, phase and frequency mutation, harmonics, etc. PLL must not be affected, and accurately track the phase and frequency of voltage positive sequence fundamental frequency component.

PLL is divided into hardware and software. Software phase locked loop is also called flexible-PLL, It can overcome the difficulties of hardware PLL, such as DC zero shift, device saturation, initialization calibration and so on. Phase locked loop (PLL) algorithm in synchronous reference frame is commonly used in three-phase system. Under the ideal voltage, the PLL can work reliably, but when the grid voltage is unbalanced or distorted, the output of the PLL will be affected, and harmonics, especially the second harmonic, will appear.

ISSN: 2414-1895 DOI: 10.6919/ICJE.202106_7(6).0073

In order to overcome the shortcomings of srf-pll in unbalanced grid voltage, DC component and high-order harmonics, decoupled dual synchronous reference frame software phase-locked loop (DDSRF-PLL) can be used. DDSRF-PLL can extract the positive and negative sequence components of grid voltage, and use decoupling network to eliminate oscillation, so as to achieve better phase-locked results. However, its algorithm structure is complex, and the low bandwidth filter still brings some delay to the system.

In order to overcome the complexity and delay of DDSRF-PLL, a software phase locked loop algorithm based on second-order generalized integrator is proposed. When the grid voltage is unbalanced, reference [15] uses equation (1) to extract the positive sequence component of the grid voltage in the two-phase static AC coordinate system.

$$v_{\alpha\beta}^{+} = \frac{1}{2}\begin{bmatrix} 1 & -q \\ q & 1 \end{bmatrix} v_{\alpha\beta} \tag{1}$$

where, q is a phase offset with a lag of 90 °, $q = e^{-j\pi/2}$.

It can be seen from equation (1) that in order to obtain the positive sequence component of the grid voltage in the $\alpha\beta$ coordinate system, it is necessary to offset the original voltage signal by 90° to obtain the two-phase orthogonal voltage. Generally speaking, the 90° phase offset based on sinusoidal signal can be achieved by periodic delay, differential and all pass filter. However, these methods are slow to respond to the change of frequency, especially the differential method is sensitive to voltage harmonics. Therefore, the 90° phase offset generated by sogi can be used to obtain two orthogonal signals. SOGI can not only realize 90° phase angle offset of power grid voltage signal, but also filter out high-order harmonics.

Firstly, this paper analyzes the traditional SOGI, points out the shortcomings of the traditional SOGI, and proposes an improved type I SOGI based on the second-order generalized integrator; in order to overcome the influence of DC component on the improved type I SOGI, an improved type II SOGI is proposed; in order to overcome the influence of high-frequency component on the improved type II SOGI, an improved type III SOGI is further proposed, which is realized by constructing the second-order generalized integrator 90° phase angle offset to generate two-phase orthogonal signal to complete the extraction of positive sequence component of power grid electrical instrument. On the basis of SOGI, an adaptive filter based on internal model principle is constructed, which can not only realize 90° phase angle offset quickly, but also filter out high-order harmonics, and realize accurate phase locking in the case of electric propulsion system containing harmonics, power grid imbalance or voltage distortion.

2. Theoretical analysis of ship harmonic detection

2.1 Traditional second order generalized integrator

The traditional sogi based orthogonal signal generator (SOGI-QSG) is shown in Figure 1, V and qV' are the two orthogonal signals of output, and ε_V is the error signal between input V and output V'.

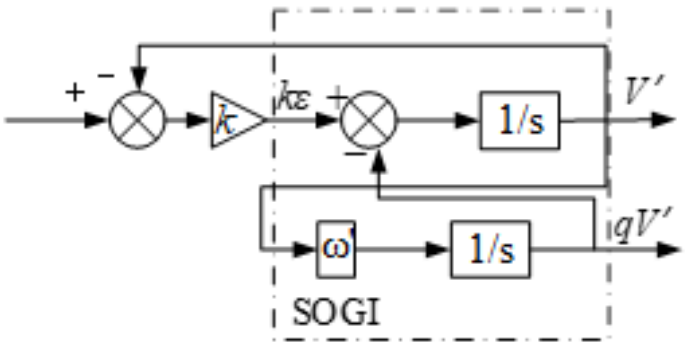

Fig. 1 Traditional SOGI structure chart

ISSN: 2414-1895 DOI: 10.6919/ICJE.202106_7(6).0073

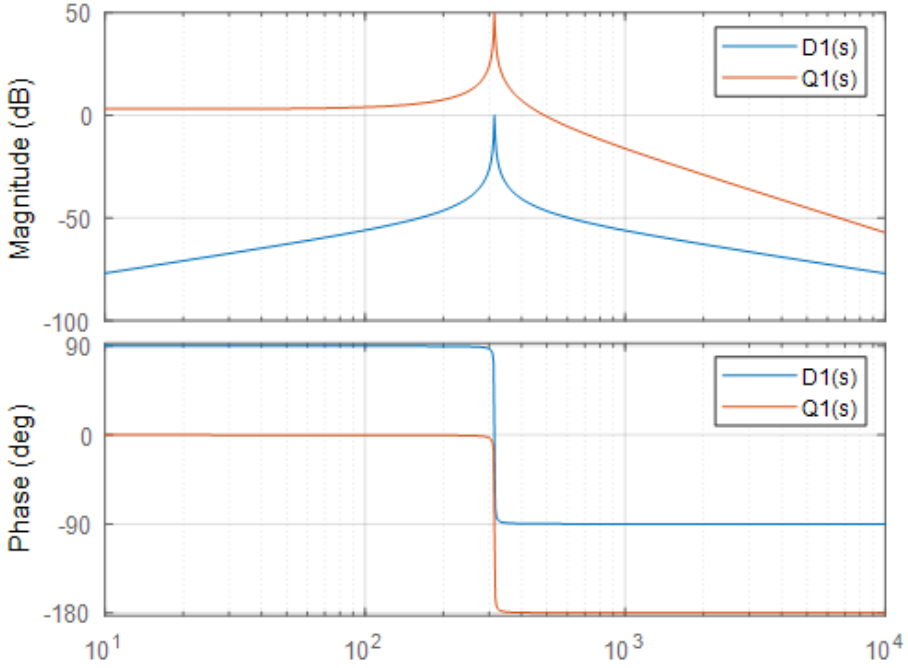

Fig. 2 Bode plot of $D_1(s)$ and $Q_1(s)$

It can be seen from the picture

$$SOGI(s) = \frac{v'}{k\varepsilon_V}(s) = \frac{\hat{\omega}s}{s^2+\hat{\omega}^2}, \tag{2}$$

$$D(s) = \frac{v'}{v}(s) = \frac{\hat{\omega}s}{s^2+k\hat{\omega}s+\hat{\omega}^2}, \tag{3}$$

$$Q(s) = \frac{qv'}{v}(s) = \frac{k\hat{\omega}^2}{s^2+k\hat{\omega}s+\hat{\omega}^2}, \tag{4}$$

Where $\hat{\omega}$ is the input resonant frequency and k is the parameter.

It is not difficult to see from equations (2) and (3) that equation (2) is a band-pass filter, and equation (3) is a low-pass filter. Their filtering performance is affected by parameter k, but independent of frequency $\hat{\omega}$. When the value of k is small, the system response is slow, but the filtering effect is good. Considering the response speed and anti-interference performance, $k = \sqrt{2}$ is selected, which corresponds to the damping coefficient $\zeta = 1/\sqrt{2}$ of the second-order system.

The bird diagram of $D_1(s)$ and $Q_1(s)$ is shown in Figure 2.

$D_1(s)$ is a second-order band-pass filter whose transfer function can be expressed as

$$D_1(s) = A_0 \frac{\frac{\omega'}{Q_{D1}}s}{s^2+\frac{\omega'}{Q_{D1}}s+\omega'^2} \tag{5}$$

Where A_0 is the gain of $D_1(s)$ and Q_{D1} is the quality factor.

$$Q_{D1} = \frac{\omega'}{k} \tag{6}$$

It can be seen from equation (6) that when k is fixed, the quality factor of $D_1(s)$ will change with the change of ω', that is, Q_{D1} will change with the fluctuation of input signal frequency, which will obviously affect the dynamic performance of the system. In order to overcome this shortcoming, an improved type I SOGI is proposed.

2.2 Improved I type ship harmonic detection second-order generalized integrator

Improved I SOGI structure as shown in figure 3, point line box part for improvement.

ISSN: 2414-1895 DOI: 10.6919/ICJE.202106_7(6).0073

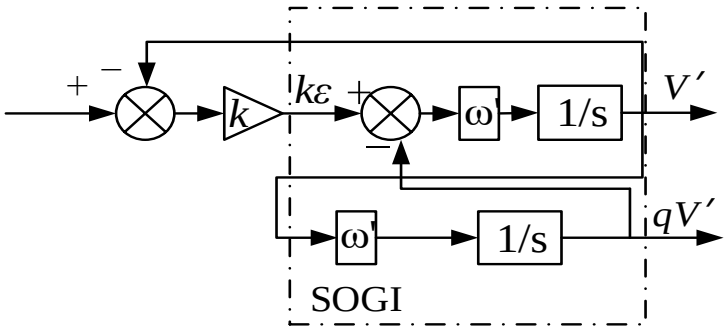

Fig. 3 Improved I-type SOGI structure chart

Type I SOGI transfer function for improvement

$$D_2(s) = \frac{V\prime(s)}{V(s)} = \frac{k\omega\prime s}{s^2+k\omega\prime s+\omega\prime^2} \tag{7}$$

$$Q_2(s) = \frac{qV\prime(s)}{V(s)} = \frac{k\omega\prime^2}{s^2+k\omega\prime s+\omega\prime^2} \tag{8}$$

$$Q_{D2} = \frac{1}{k} \tag{9}$$

Obviously, the quality factor of improved type I SOGI is not affected by frequency ω'. By comparing equation (6) with equation (9), it is found that $Q_{D2} < Q_{D1}$ indicates that the improved type I SOGI has a wider passband, so it is easier to make the system stable in the phase-locked process. In order to further illustrate the difference between traditional SOGI and improved type I SOGI, $D_1(s)$ and $D_2(s)$ are compared and analyzed by Bode diagram, as shown in Figure 4. As can be seen from Figure 4, the passband of $D_1(s)$ is narrow, and it is highly frequency dependent, but the filtering effect is good; the passband of $D_2(s)$ is wide, and its frequency dependence is obviously less than that of $D_1(s)$, but the filtering effect is poor.

Under different values of k, the Bode diagrams of $D_2(s)$ and $Q_2(s)$ transfer functions in the improved type I SOGI are shown in Fig. 5 and Fig. 6.

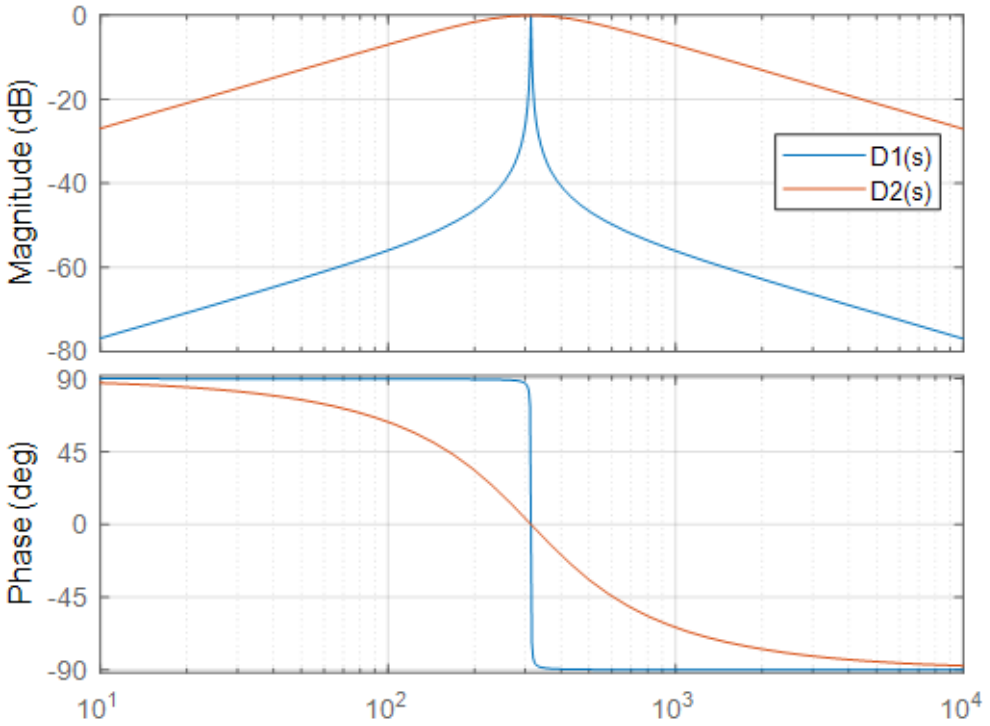

Fig. 4 Bode plot of $D_1(s)$ and $D_2(s)$

ISSN: 2414-1895 DOI: 10.6919/ICJE.202106_7(6).0073

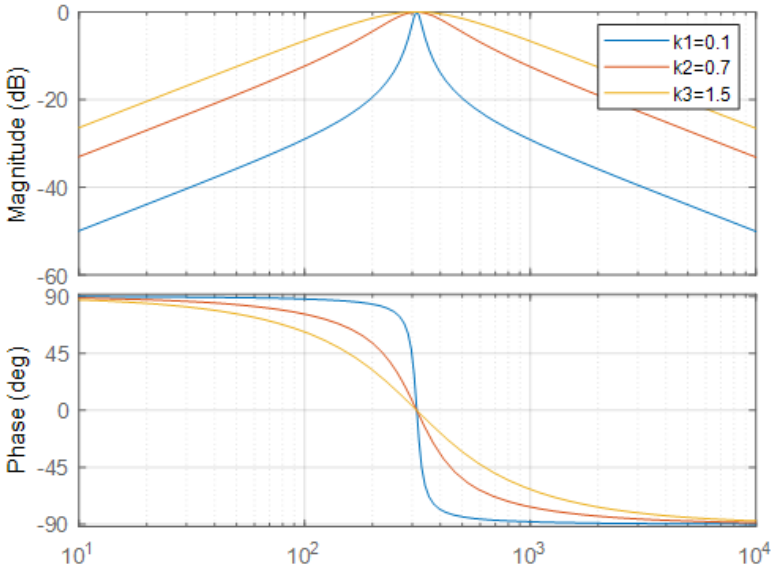

Fig. 5 Bode plot $D_2(s)$ of improved I-type SOGI

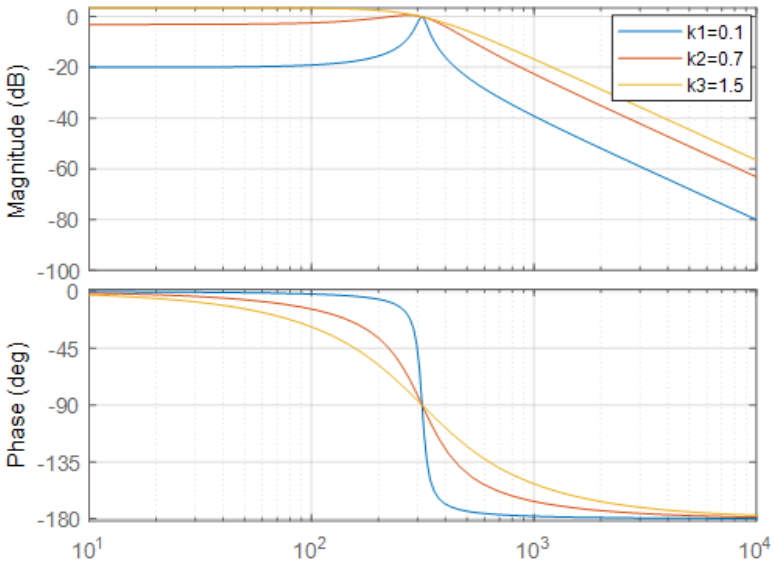

Fig. 6 Bode plot $Q_2(s)$ of improved I-type SOGI

As can be seen from Figure 5, $D_2(s)$ is a second-order band-pass filter, and its frequency bandwidth is only affected by the value of k, independent of the resonant frequency ω'. except for the center frequency ω', other frequencies will have great attenuation. It can be seen from Figure 6 that $Q_2(s)$ represents a low-pass filter, and its steady-state gain is also only affected by k, independent of resonant frequency ω'. The bandwidth can be set by adjusting the value of k. The smaller the value of k, the better the filtering effect of the filter, but the longer the dynamic response time.

For k value, considering the filtering effect and response speed of sogi, generally k is near $\sqrt{2}$, which is consistent with the quality factor $Q_{D2} = 0.707$ of the filter.

2.3 Improved II type ship harmonic detection second-order generalized integrator

According to the attenuation characteristics of $D_2(s)$ pair of DC components, $D_2(s)$ can filter out all the DC components in the input signal v, that is to say, the output of D does not contain DC components. From the structure diagram, v' can eliminate DC components through negative feedback to the input signal. As can be seen from Figure 6, $Q_2(s)$ is a low-pass filter. Once there is any DC component in the input signal v, the output signal qv' is easily affected by the DC voltage

ISSN: 2414-1895 DOI: 10.6919/ICJE.202106_7(6).0073

signal offset, which leads to the error in the amplitude detection of the input voltage signal and affects the subsequent phase angle locking. Therefore, an improved type II sogi is proposed.

The structure diagram of the improved type II SOGI is shown in Figure 7. The improved part in the left dotted line box for eliminating the DC component.

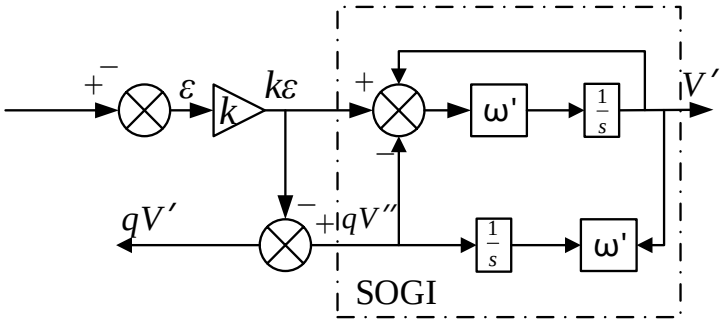

Fig. 7 Improved II-type SOGI structure chart

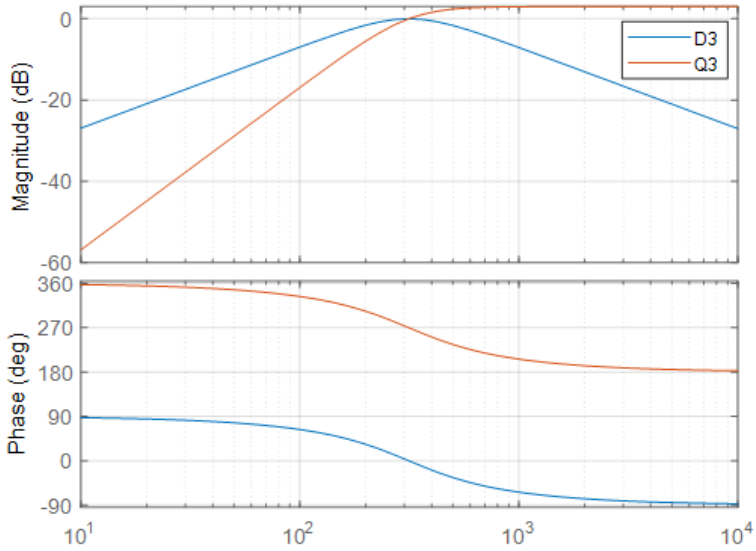

Fig. 8 Bode plot of $D_3(s)$ and $Q_3(s)$

According to the above analysis, the output signal v' does not contain any DC component. If the input signal v contains DC component, then after the negative feedback of the output signal v', ε contains the same DC component as the input signal v. after the gain k is amplified, the signal is subtracted from qv'' to eliminate the DC component in qv'.

According to figure 7, the transfer functions of $D_3(s)$ and $Q_3(s)$ are as follows

$$D_3(s) = \frac{v'(s)}{v(s)} = \frac{k\omega' s}{s^2 + k\omega' s + \omega'^2} \tag{10}$$

$$Q_3(s) = \frac{qv'(s)}{v(s)} = -\frac{ks^2}{s^2 + k\omega' s + \omega'^2} \tag{11}$$

$D_3(s)$ is the same as $D_2(s)$, $Q_3(s)$ has changed, and the Bode diagrams of $D_3(s)$ and $Q_3(s)$ are shown in Figure 8. As can be seen from figure 8, the output characteristics of $D_3(s)$ of the improved type II sogi are the same as that of $D_2(s)$ of the improved type I SOGI, while the output characteristics of $Q_3(s)$ have changed. The gain in the low frequency band is a large negative number, which can filter out the DC component in qv', so that there is no DC component in output qv', However, with the increase of frequency, the gain of $Q_3(s)$ increases gradually, which leads to the decrease of the ability of the improved transfer function $Q_3(s)$ to suppress high frequency noise.

ISSN: 2414-1895 DOI: 10.6919/ICJE.202106_7(6).0073

2.4 Improved III type ship harmonic detection second-order generalized integrator

The improved type I SOGI has a weak ability to suppress DC component. In order to overcome the disadvantage that the output result of the improved type II SOGI is biased due to the DC component of the input signal, $k\varepsilon$ is directly introduced into qv'' to make it contain high-frequency harmonics. Therefore, this paper proposes a third improved sogi, that is, adding a low-pass filter to the improved type III SOGI to filter out higher harmonics. The improved type III SOGI has all the advantages of the improved type I and type II, and has the ability to suppress the DC component and high-order harmonic component of the input signal. Its structure is shown in Figure 9.

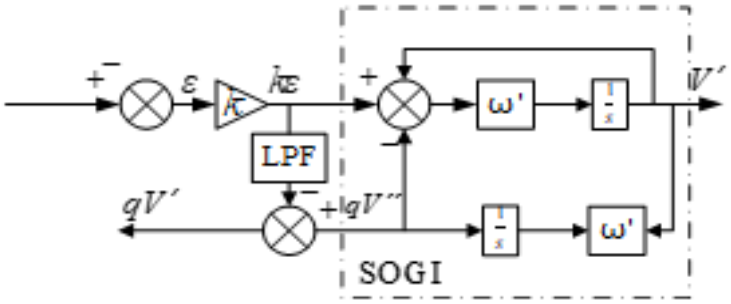

Fig. 9 Improved III-type SOGI structure chart

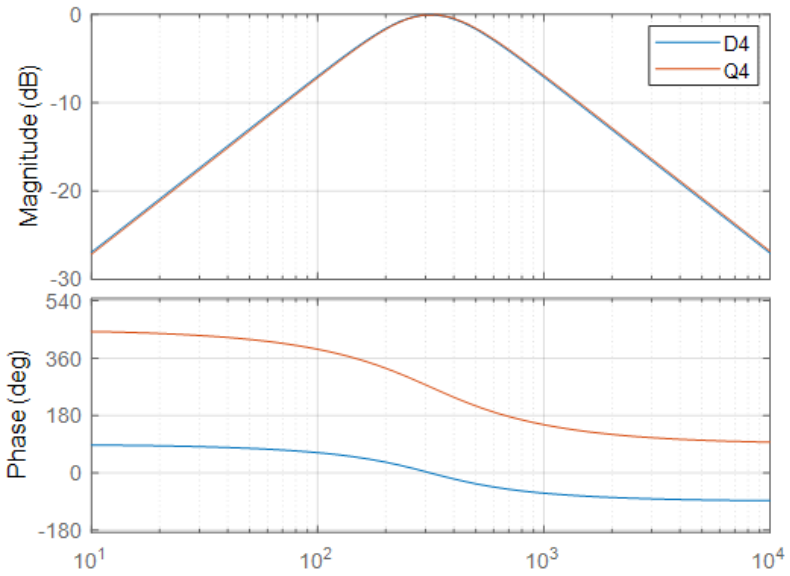

Fig. 10 Bode plot of $D_4(s)$ and $Q_4(s)$

It can be seen from Figure 9 that the improved type III sogi adds a low-pass filter (LPF) to the channel where $k\varepsilon$ and qv'' are subtracted. The addition of low-pass filter can make qv' have a larger attenuation in the high frequency band, The LPF transfer function is as follows

$$G_{LPF}(s) = \frac{1}{1+\tau s} \tag{12}$$

Where τ is related to the cut-off frequency of LPF.

qv' is to get 50 Hz sinusoidal signal, so the cut-off frequency of LPF can be selected at 50 Hz. According to figure 9, $D_4(s)$ and the transfer function are

$$D_4(s) = \frac{v'(s)}{v(s)} = \frac{k\omega' s}{s^2+k\omega' s+\omega'^2} \tag{13}$$

$$Q_4(s) = \frac{qv'(s)}{v(s)} = -\frac{k(\tau\omega'^2 s-s^2)}{(s^2+k\omega' s+\omega'^2)(1+\tau s)} \tag{14}$$

ISSN: 2414-1895 DOI: 10.6919/ICJE.202106_7(6).0073

$D_4(s)$ is the same as $D_2(s)$ and $D_3(s)$, and its performance is the same; $Q_4(s)$ is more complex than $Q_2(s)$ and $Q_3(s)$, but its performance has been improved to a certain extent. The Bode diagram of $D_4(s)$ and $Q_4(s)$ is shown in Figure 10.

It can be seen from Fig. 10 that the amplitude frequency characteristics of $Q_4(s)$ are basically the same as that of $D_4(s)$ after adding LPF, that is to say, $Q_4(s)$ can not only suppress the DC component in the signal, but also suppress the high frequency component in the input signal well, and there is no delay at the fundamental frequency due to the addition of LPF, which is the comprehensive performance of improved type I and improved type II, and has the advantages of the two improved types at present.

3. Design of improved SOGI harmonic detection PLL for ship propulsion system

SOGI-PLL firstly obtains v_α and v_B by Clarke transform of three-phase grid voltage signal v_a, v_b, v_c, then obtains two groups of orthogonal fundamental signals v'_α and qv'_α and v'_B and qv'_B by two SOGI, then extracts the fundamental positive sequence components v_α^+ and v_B^+ of grid voltage signal by positive sequence component calculation, and obtains q-axis component v_q^+ by park transform, finally phase-locked by SFR control mode. The structure of the new SOGI-PLL harmonic detection PLL for ship propulsion system is shown in Figure 11.

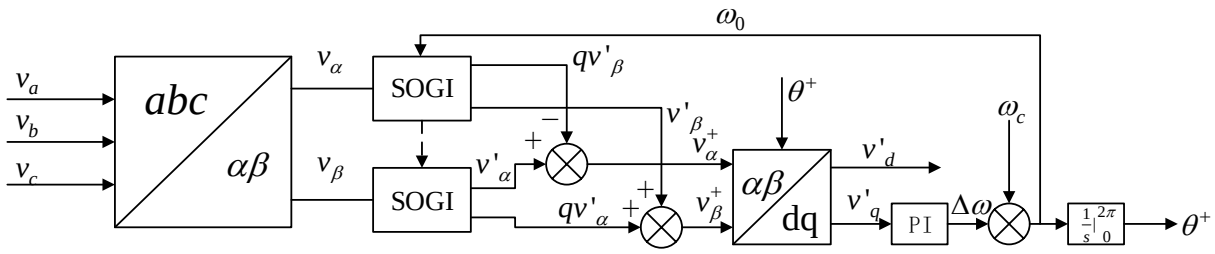

Fig. 11 SOGI-PLL block diagram

Phase angle ω_0 is introduced in the figure, as shown by the dotted line. The whole phase-locked process has adaptive function. When the frequency of power grid voltage signal changes, the phase-locked loop can accurately track the frequency of power grid voltage. The purpose of adding ω_c is to speed up the adjustment speed of PLL. If PI control is used instead, it will cause the overshoot of ω_0 and lead to the instability of the system.

The fundamental positive sequence component extracted from the grid voltage signal is

$$v_\alpha^+ = v'_\alpha - qv_B^+ \tag{15}$$

The signal orthogonal to 1 is

$$v_B^+ = qv'_\alpha + v'_B \tag{16}$$

It can be seen from equations (15) and (16) that the positive sequence component v_α^+ is related to v'_α and qv'_B, while the orthogonal component v_B^+ is related to qv'_α and v'_B. From the above analysis, it can be seen that the output qv'_α and qv'_B of the improved type I SOGI are easily affected by the DC component of the grid voltage signal, and the output qv'_α and qv'_B of the improved type II SOGI are easily affected by the higher harmonics. Under different grid voltage conditions, as long as the accuracy of qv'_α and qv'_B is ensured, v_α^+ is the fundamental positive sequence component of v_α in the grid voltage signal, so as to ensure the accuracy of phase locking.

Three kinds of improved SOGI-PLL will get different phase-locked results under different grid voltage conditions. Improved type I SOGI-PLL: when the grid voltage contains DC component, the phase-locked results will have errors. Improved type II SOGI-PLL: when the grid voltage has higher harmonics, the phase-locked result will have error. Improved type III SOGI-PLL: when the grid

ISSN: 2414-1895 DOI: 10.6919/ICJE.202106_7(6).0073

voltage contains high harmonic and DC component, the error of phase-locked result is very small. The PI regulated SOGI-PLL will not be described in detail.

4. Simulation analysis

In this paper, Matlab / Simulink software is used to simulate and verify the improved type I SOGI-PLL, improved type II SOGI-PLL and the improved type III SOGI-PLL algorithm proposed in this paper under the conditions of three-phase voltage symmetry, three-phase voltage asymmetry, frequency mutation, phase mutation and harmonic. In the improved DSOGI-PLL algorithm, $k = \sqrt{2}$. The simulation results are as follows: ① Three phase symmetry of grid voltage; ② The grid voltage is unbalanced, phase A is voltage rating, phase B and phase C are unbalanced; ③ The grid voltage contains higher harmonics.

4.1 Three phase symmetry of grid voltage

Under the condition of grid voltage balance, the comparative test waveforms of the three schemes are analyzed. The output results of the three improved SOGI-PLL are consistent, and the phase angle θ^+ obtained by phase-locked is almost consistent, which can accurately track the phase of grid voltage. This shows that the three improved SOGI-PLL have reliable phase-locked accuracy.

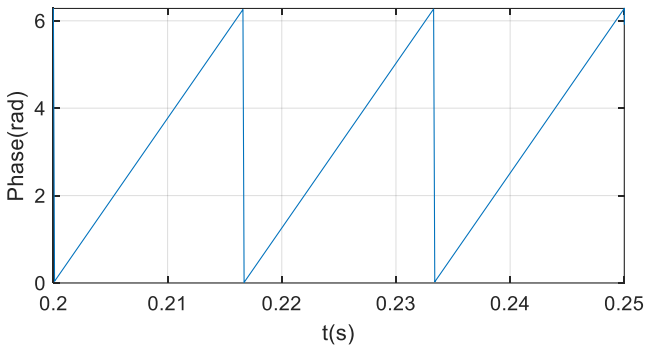

Fig. 12 Improved type I phase lock diagram

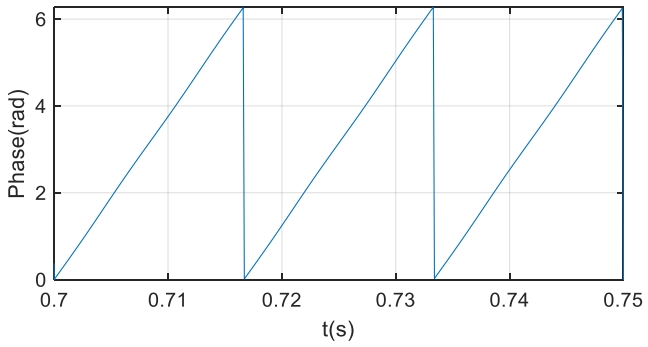

Fig. 13 Improved type II phase lock diagram

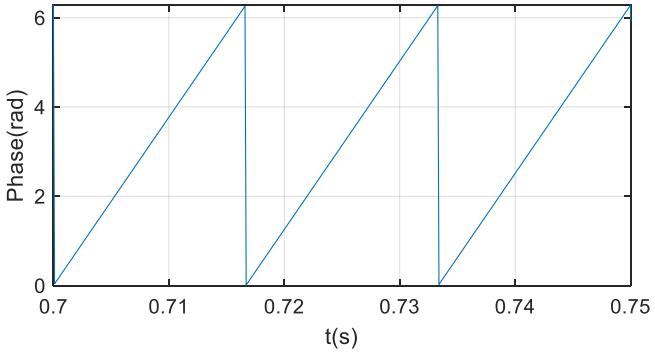

Fig. 14 Improved type III phase lock diagram

ISSN: 2414-1895 DOI: 10.6919/ICJE.202106_7(6).0073

4.2 Unbalanced grid voltage

Figure 14 shows the comparative simulation waveforms of three improved SOGI-PLL when the grid voltage is A-phase balanced and B-phase and c-phase unbalanced. It can be seen that when the improved type I sogi is used as the PLL positive sequence fundamental extraction unit, v_α^+ and v_B^+ are unbalanced, and the q-axis component fluctuates after the park transform, resulting in the deviation of phase-locked angle θ^+.

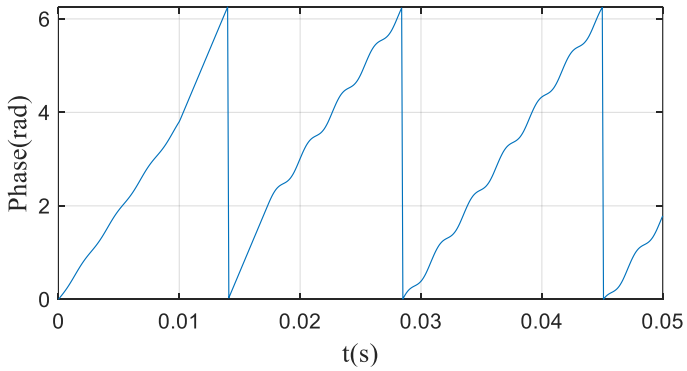

Fig. 15 Improved type I phase lock diagram

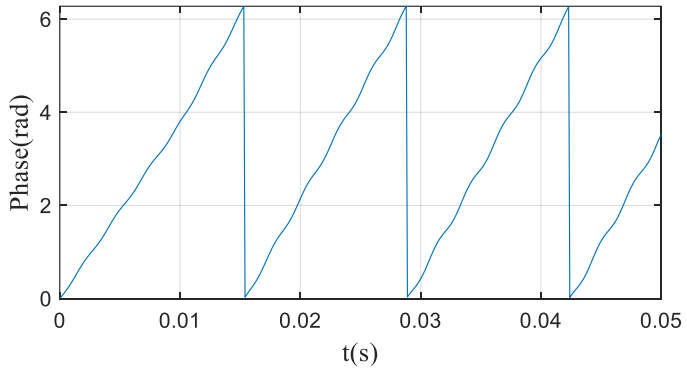

Fig. 16 Improved type II phase lock diagram

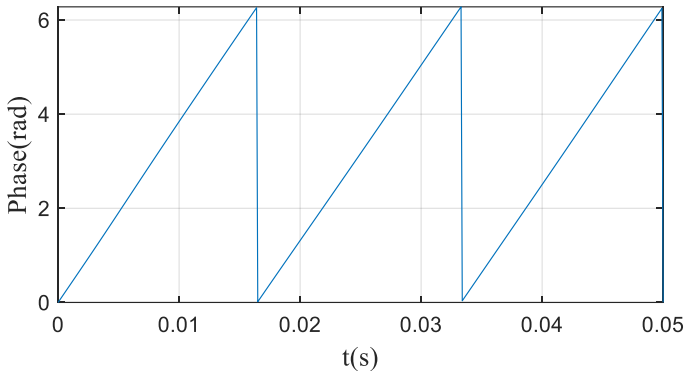

Fig. 17 Improved type III phase lock diagram

4.3 The grid voltage contains harmonics

The following figure shows the comparative simulation waveforms of three improved SOGI when the power grid contains harmonics. The improved type II and improved type III have the ability to suppress high-order harmonics, and the phase-locked angle θ^+ can accurately track the positive sequence component of fundamental wave. Due to the weak suppression ability of the improved type I SOGI to the higher harmonics, the higher harmonics will be superimposed on the v_B^+ and the error of the phase lock angle θ^+ will appear.

ISSN: 2414-1895 DOI: 10.6919/ICJE.202106_7(6).0073

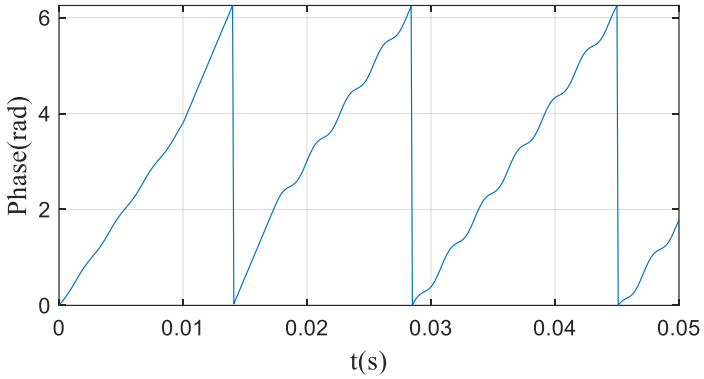

Fig. 18 Improved type I phase lock diagram

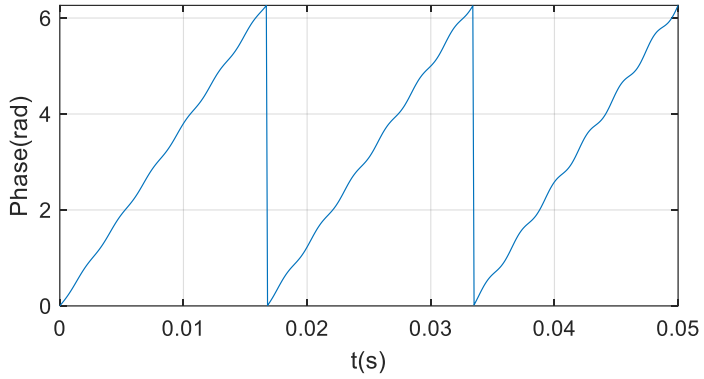

Fig. 19 Improved type II phase lock diagram

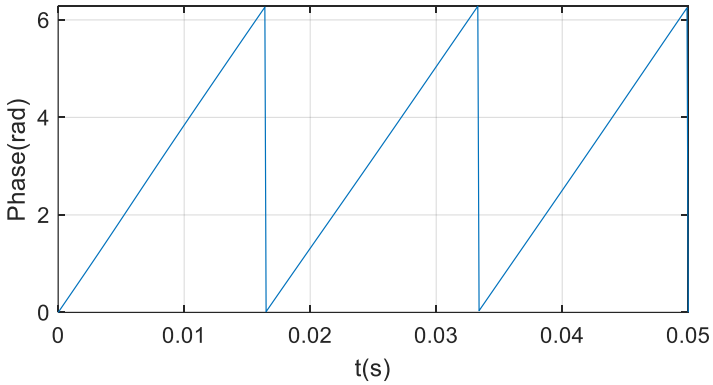

Fig. 20 Improved type III phase lock diagram

5. Conclusion

In this paper, three improved structures are proposed for the defects of the general SOGI, and the three improved SOGI are analyzed theoretically. After applying the three improved SOGI to PLL, it can be seen that when the grid voltage is symmetrical, the three improved SOGI-PLL can accurately track the voltage phase; when the grid voltage is not equal, the improved type II and type III SOGI-PLL can accurately output the phase-locked results; when the grid voltage contains harmonics, the phase-locked effect of the improved type III SOGI-PLL is the best.

Acknowledgments

This works is supported by a fund project: The Shanghai Science and Technology Committee (STCSM) Project (Project Name: Research on Intelligent self-healing of ship regional distribution power system, Project No.: 20040501200).

ISSN: 2414-1895 DOI: 10.6919/ICJE.202106_7(6).0073

References

[1] D. Velasco C. Trujillo G. Garcera and E. Figueres "An active anti-islanding method based on phase- PLL perturbation" IEEE Trans. Power Electron. vol. 26 no. 4 pp. 1056-1066 Apr. 2015.

[2] S. Golestan M. Monfared F. Freijedo and J. Guerrero "Design and tuning of a modified power-based PLL for single-phase grid-connected power conditioning systems" IEEE Trans. Power Electron. vol. 27 no. 8 pp. 3639-3650 Aug. 2017.

[3] M. Karimi-Ghartemani, "A Unifying Approach to Single-Phase Synchronous Reference Frame PLLs," in IEEE Transactions on Power Electronics, vol. 28, no. 10, pp. 4550-4556, Oct. 2013, doi: 10.1109/ TPEL. 2016.2235185.

[4] T. Thacker D. Boroyevich R. Burgos and F. Wang "Phase-locked loop noise reduction via phase detector implementation for single-phase systems" IEEE Trans. Ind. Electron. vol. 58 no. 6 pp. 2482-2490 Jun. 2013.

[5] S.-H. Hwang L. Liu and J.-M. Kim "DC offset error compensation for synchronous reference frame PLL in single-phase grid-connected converters" IEEE Trans. Power Electron. vol. 27 no. 8 pp. 3467-3471 Aug. 2012.

[6] M. Karimi-Ghartemani S. Khajehoddin P. Jain and A. Bakhshai "Derivation and design of in-loop filters in phase-locked loop systems" IEEE Trans. Instrum. Meas. vol. 61 no. 4 pp. 930-940 Apr. 2012.

[7] S. da Silva L. Campanhol A. Goedtel C. Nascimento and D. Paio "A comparative analysis of p-PLL algorithms for single-phase utility connected systems" Proc. 13th IEEE Eur. Conf. Power Electron. Appl. pp. 1-10 2019-Sep.

[8] Y. Wang and Y. Li "Grid synchronization PLL based on cascaded delayed signal cancellation" IEEE Trans. Power Electron. vol. 26 no. 7 pp. 1987-1997 Jul. 2011.